

Normal asynchrony of left ventricular long and short axes: Their relationship with aortic hemodynamics

Chloe M.L. Page^a, Ashraf W. Khir^a, Alun D. Hughes^b, Robin Chung^c, Michael Y. Henein^{d,*}

^a Brunel Institute for Bioengineering & School of Engineering and Design, Brunel University, Uxbridge, Middlesex UB8 3PH, UK

^b International Centre for Circulatory Health, St. Mary's Hospital & Imperial College, Paddington, London, UK

^c Echocardiography Department, Royal Brompton Hospital, London SW3 6NP, UK

^d Heart Centre, Umea University Hospital, Sweden

Received 16 October 2008; accepted 14 December 2008

Available online 23 February 2009

Abstract

Background: The relationship between left ventricular (LV) long and short axes, aortic pressure (P), flow velocity (U) and wave intensity is not well established.

Methods: Eleven dogs were anaesthetized and mechanically ventilated and LV long and minor axes shortening velocities were calculated using ultrasound crystals. P and U were measured in the ascending aorta using a high fidelity pressure catheter and ultrasonic flow transducer.

Results: Pre-ejection: The LV minor axis began to shorten as the long axis lengthened creating LV shape change. Early ejection: The aortic valve opened 83 ± 20 ms after the ECG Q-wave. Aortic P and U simultaneously increased; peak aortic velocity and maximum minor axis shortening velocity (M_{\max}) occurred at 152 ± 24 and 147 ± 24 ms, respectively; $p=0.66$, intra-class correlation ICC 0.93). M_{\max} also corresponded to the time when the reflected compression wave arrived back to the heart (ICC 0.75). Late ejection: LV long axis reached its peak shortening velocity 28 ± 21 ms later than the minor axis at 175 ± 33 ms, coinciding with peak LV pressure (187 ± 25 ms; $p=0.77$, ICC 0.65) and onset of the forward expansion wave (177 ± 28 ms, $p=0.88$, ICC 0.89). Both axes then continued to slow until 210 ± 30 ms when an increased rate of decline of shortening velocity corresponded with peak aortic pressure.

Conclusion: Long axis peak shortening velocity lagged consistently behind the minor axis, representing a degree of normal asynchrony. The arrival of the reflected wave appears to bring about the slowing down of the minor axis.

© 2008 Elsevier Ireland Ltd. All rights reserved.

Keywords: Asynchrony; Wave intensity; Left ventricular fibre architecture

1. Introduction

Ultrasound techniques have revolutionized our understanding of cardiac physiology in health and disease. The ability to provide detailed information on events during various phases of the cardiac cycle has enabled optimum management strategies for different cardiac conditions.

Furthermore, studying cardiac physiology in the light of its anatomical basis is of immense importance in this respect. Left ventricular systole occurs due to the contraction of its two myocardial components, circumferential which occupies the basal and mid-cavity regions, as well as the longitudinal which occupies mainly the subendocardial and to a lesser extent the subepicardial layers [1]. Contraction of these two myocardial components results in shortening of the minor and long axes, respectively, increased intraventricular pressure, opening of the aortic valve and blood ejection. Closure of the aortic valve marks end-ejection and the onset of diastolic phases.

* Corresponding author. Heart Centre, Umea University Hospital, Sweden.

E-mail address: michael.henein@medicin.umu.se (M.Y. Henein).

Efficient function of the LV is achieved by coherent behavior of the two axes. Although time relations of the onset of long and minor axis shortening have been studied [2] further details about their velocity relations is lacking. Furthermore, little is known about the direct association between the long and minor axes and the product of overall ventricular systolic function i.e. aortic pressure and velocity events. Finally, potential relationships between mechanical ventricular function of the two axes and aortic waves studied by wave intensity analysis have not yet been reported. The aim of this study therefore was to investigate the relationship between ventricular systolic function as demonstrated by its long and minor axes, aortic ejection events and aortic waves.

2. Materials and methods

2.1. Animal experiment

Eleven open chest mongrel dogs were anaesthetised by 30 mg/kg body weight of i.v. sodium pentobarbital, and a maintenance dose of 75 mg/h for the duration of the experiment. The forelegs and left back legs of the dogs were connected to an electrocardiogram through three electrodes. The dogs were intubated and mechanically ventilated using constant volume ventilation (Model 607, Harvard Apparatus Company, Millis, MA, USA). The baseline heart rate was 87 ± 11 beats per minute equating to a mean RR-interval of 710 ± 83 ms.

2.1.1. LV axis measurements

Two pairs of 5 MHz ultrasound sonomicrometer crystals (Sonometrics, Ontario, Canada) were embedded into the left ventricular myocardium to measure minor and long axis movements during the cardiac cycle. One pair recorded left ventricular long axis movement from base to apex and the other pair recorded the minor axis movement from the septum to the free wall. Long and minor axis velocities were calculated by differentiating the amplitude of movement with respect to time.

2.1.2. LV pressure measurements

LV pressure was measured using a high-fidelity pressure catheter (Millar Instruments inc, Houston, TX, USA) inserted into either the brachial or carotid artery and fed down through the aortic valve into the LV or directly through the left atrium passing through the mitral valve into the LV cavity.

2.1.3. Aortic pressure and velocity measurements

Aortic pressure and velocity were measured simultaneously. Aortic root pressure (approximately 1 cm distal to the valve) was recorded using a high-fidelity pressure catheter (Millar Instruments inc., Houston, TX, USA). A mercury manometer was used to calibrate the pressure catheter before each experiment. Aortic flow velocity was measured using an ultrasonic flow probe (model T201, Transonic Systems Inc.,

Ithaca, NY, USA) that was positioned onto the ascending aorta, approximately 1 cm distal to the aortic valve.

Blood flow and pressure recordings were made for 30 s. The data was recorded at a 200 Hz sampling rate and baseline aortic U and P were plotted in Matlab and aligned by eye before analysis (as the transducers have different phase responses). To agree with the maximum lag caused by the filter in the ultrasonic flow meter, shifting of 3 or less sampling intervals was necessary in some cases.

2.1.4. Aortic wave analysis

A comprehensive account of wave intensity analysis is given in earlier papers [3,4]. Wave intensity is a measure of the energy carried by the wave. It is calculated by multiplying infinitesimal changes in pressure and velocity. A positive value represents a forward wave and a negative value represents a reflected wave. Derivation of wave intensity (dI) is based on the solution of the 1-D conservation of mass and momentum equations and is defined as the rate of energy flux per unit area (W/m^2).

$$dI = dPdU \quad (1)$$

where dP and dU are the pressure and blood velocity differentials.

When wave speed is known forward and backward wave intensity can be described in terms of measured pressure and velocity using the following equation,

$$dI_{\pm} = \pm 1/4\rho c(dP \pm \rho c dU)^2 \quad (2)$$

where ρ is density of the blood 1050 kg/m^3 , and c is wave speed.

2.1.5. LV wall movement

LV long and minor axis dimensions were measured simultaneously from the same cardiac cycle. The onset of long and minor axis shortening was measured with respect to the Q wave of the superimposed electrocardiogram. LV long and minor axis shortening velocities were computed by differentiating the amplitude of the movement with respect to time. LV axes shorten in two phases: ‘fast shortening’ (acceleration) until they reach the maximum rate of shortening ($L_{\max U}$ and $M_{\max U}$ measured in cm/s, followed by a ‘slow shortening’ phase (deceleration), where the axes are still shortening but at a reduced velocity (Fig. 1).

2.1.6. Velocity and pressure

Velocity: The timing of peak aortic blood velocity (U_{\max}) was measured with respect to the peak of the Q wave of the electrocardiogram ($t=0$).

Aortic pressure: The timing of peak measured aortic pressure (P_{\max}) was recorded. The first derivative of the aortic pressure curve (dP_A/dt) was additionally determined throughout the duration of the cycle.

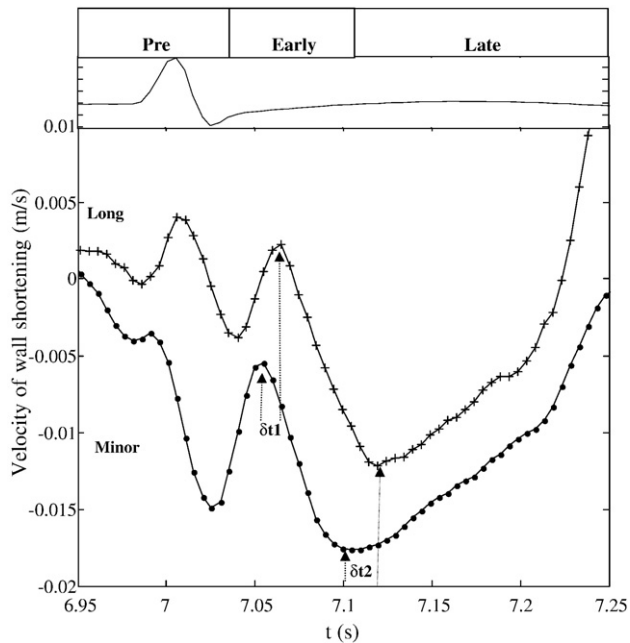


Fig. 1. Shortening velocity of the long (+) and minor (●) axes during the three ejection phases. Notice that during pre-ejection the minor axis is shortening while the long axis is lengthening. The long axis starts to shorten 30 ms after the minor axis during early ejection (δt_1) and reaches its peak shortening velocity 30 ms after that of the minor axis (δt_2). The starts represent a time in late ejection when both axes change their rate of shortening for the second time which corresponds to peak aortic pressure.

LV pressure: The timing of peak LV pressure (LV_{max}) was recorded and LV dP_{LV}/dt throughout the cycle was calculated to determine the time of peak dP_{LV}/dt during pre-ejection.

2.1.7. Wave intensity analysis

A typical wave intensity plot measured in the aortic root is dominated by a forward wave at the beginning and the end of ejection and one reflected wave during mid-systole. The forward wave during early systole is a compression wave associated with a positive dP_A/dt . The second forward wave in late systole is an expansion wave [3] associated with a negative dP_A/dt . The reflected wave is a backward compression wave that is associated with a positive dP_A/dt but decelerates aortic flow. The net waves are the summation of the forward and backward waves, so in order to see the exact timings of the forward and backward waves we also separated the wave intensity.

2.1.8. Statistical analysis

A representative cycle for each dog was chosen during steady state. The times for each hemodynamic parameter were calculated by averaging all 11 dogs times to establish a sequence of events. Statistical analysis was performed with the statistical package SPSS. Data are expressed as mean \pm SD. CVSOFT (Odessa Computer Systems Ltd, Calgary, Canada) was used to transform the data into ASCII format in order to be analysed using Matlab (The MathWorks Inc., MA, USA) programs. LV wall motion, aortic pressure and blood velocities

as well as wave intensity analysis were studied and their timings were calculated. Agreement between measures is presented as mean difference (SD of difference) and was quantified using Lin's concordance coefficient (intra class correlation) [5].

3. Results

Systole was divided into three stages: pre-ejection (from deflection of electrocardiogram Q-wave to aortic valve opening and onset of aortic flow), early ejection (up to and including the peak of ejection, taken as peak velocity) and late ejection (following the peak of ejection). Events occurring during each phase were grouped together to simplify presentation of analysis.

3.1. Phase 1: pre-ejection

During pre-ejection the LV minor axis began to shorten, the peak velocity of minor axis shortening during this phase occurred at 37 ± 20 ms, thereafter the velocity of shortening declined until opening of the aortic valve. Minor axis shortening was accompanied by lengthening of the long axis which reached a peak velocity at 51 ± 20 ms and subsequently declined Fig. 1. This phase ended with the opening of the aortic valve at 83 ± 20 ms which closely followed peak dP_{LV}/dt (78 ± 20 ms) by a few milliseconds and ejection commenced.

3.2. Phase 2: early ejection

After opening of the aortic valve the minor axis underwent a second period of shortening. In contrast, the long axis initially showed a small increase in length after opening of the aortic valve but subsequently began to shorten at 114 ± 20 ms. The commencement of long axis shortening during early ejection therefore lagged minor axis shortening by ~ 30 ms. Fig. 1 (δt_1). Both minor and long axes then continued to shorten rapidly during early ejection. Aortic pressure and velocity simultaneously increased during early-ejection resulting in a forward compression wave in the aorta. Peak dP_A/dt was reached 110 ± 30 ms after the onset of ejection, just prior to the peak of the compression wave. The time of peak ejection velocity (U_{max}) and the maximum shortening velocity of the minor axis (M_{max}) occurred together at 152 ± 24 and 147 ± 24 ms, respectively. At this time the long axis continued to shorten at increasing velocity (Fig. 1). The time association between minor axis velocity and peak ejection velocity was very strong (ICC 0.93) with no significant time difference in their coincidence ($p=0.66$) (Fig. 2). The time of maximum shortening of the minor axis also coincided with the onset of reflected compression wave with no significant time difference (ICC 0.75) (Fig. 3).

3.3. Phase 3: late ejection

During late ejection the velocity of shortening of the LV long axis increased until eventually reaching its peak

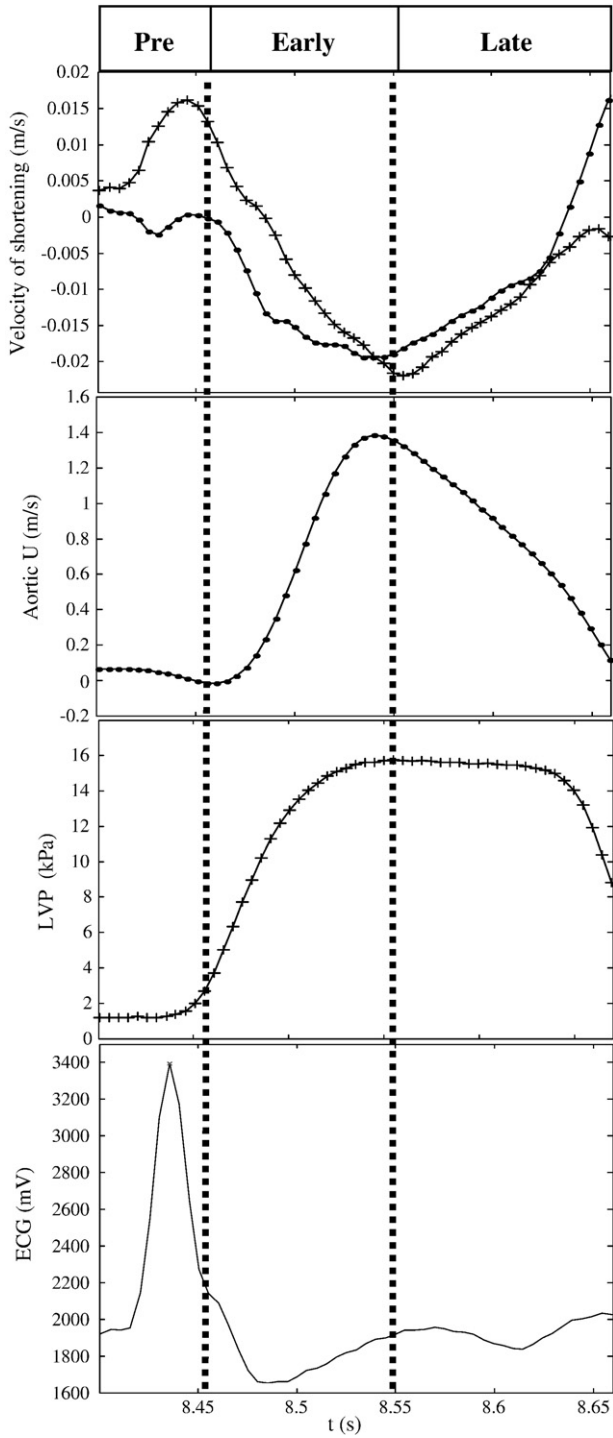


Fig. 2. A composite showing the hemodynamic events that occur in phase with LV wall movement. It shows that the minor axis reaches its maximum shortening velocity at the same time as peak aortic flow, and the long axis reaches its maximum shortening velocity at the same time as peak LV pressure.

shortening velocity (L_{max}) $28 + 21$ ms later than the minor axis at 175 ± 33 ms. Fig. 1 ($\delta 2$). L_{max} corresponded strongly with LV peak pressure (Fig. 2) and with the onset of the forward expansion wave (dI_{+e}) Fig. 3, (L_{max} $175 + 33$ v LVP_{max} $187 +$

25 ms, $p=0.33$, ICC 0.65; dI_{+e} $177 + 28$ ms, $p=0.88$, ICC 0.89). Very late in systole, 210 ± 30 ms after the Q-wave as the axes were slowing, we observed an increased rate of decline of velocity of shortening of both axes which corresponded with the rapid decline of aortic pressure Fig. 1. End-ejection coincided with the dicrotic notch of the aortic pressure wave and end of the forward expansion wave (Fig. 4).

4. Discussion

4.1. Findings

In this study we have found that close time relations exist between LV mechanical function as shown by the shortening

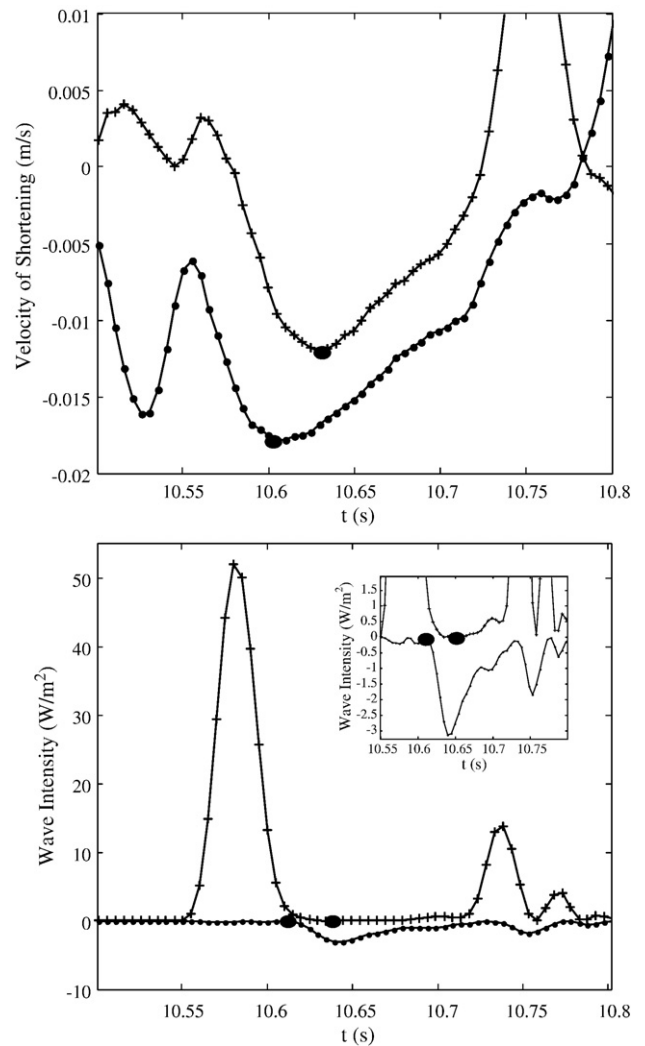


Fig. 3. A composite showing the relationship between LV wall movement and wave intensity analysis. The minor axis begins to slow at the time of return of the reflected compression wave in mid-systole. Long axis shortening begins to slow later and produces a decline in LV pressure which generates the forward expansion wave, the times of these events are represented by the corresponding black dots. The enlarged Y-axis of wave intensity shows the true onset of the forward expansion wave.

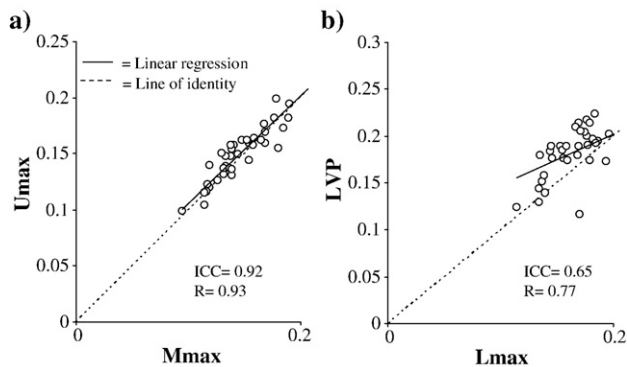


Fig. 4. Concordance plots of a) U_{\max} (time of peak aortic velocity) and M_{\max} (time of maximum minor axis velocity). Concordance coefficient=0.92; Pearson's $r=0.93$, and b) Concordance plot of LVP_{\max} (time of LV max pressure) and L_{\max} (time of maximum long axis velocity). Concordance coefficient=0.65; Pearson's $r=0.77$.

of its long and short axes and events of aortic ejection namely, pressure, velocity and aortic waves. LV minor axis peak shortening velocity occurs within 150 ms from the onset of depolarisation (Q-wave), coinciding with peak aortic velocity and the arrival of the reflected wave. Long axis peak shortening velocity consistently lags by 30 ms behind the minor axis and coincides with peak LV pressure and onset of the expansion wave which leads to aortic pressure decline.

4.2. Mechanisms

Peripheral tissue perfusion which determines exercise activities as well as all pan organ physiology depends on the cardiac output which itself depends on the stroke volume [6]. With a fixed LV outflow tract cross sectional area the stroke volume is determined by efficiency of LV contraction as well as optimum ejection times. In this study we have demonstrated that ejection events are determined by the normal relationship between the two contracting axes of the LV, long and minor. Minor axis peak shortening velocity coincides with the arrival of the reflected wave. Long axis peak shortening velocity lagged behind that of the minor axis by 30 ms representing a degree of physiologically normal asynchrony between the two components of LV systolic function. This is not a faulty design of the heart, but delayed peak long axis shortening is meant to maintain the LV pressure for a further 30 ms, after which it starts to decline at the time of the onset of the forward expansion wave. Finally, as long axis shortening velocity decline is completed the aortic valve closes, followed by continuing pressure decline during the isovolumic relaxation period of the cardiac cycle.

4.3. Data interpretation

Early studies of LV synchronous function by Wiggers highlighted evidence for 'fractionate contractions' [7]. This has recently been demonstrated by studying the two com-

ponents of ventricular function; long and minor axes [8]. They are complementary contributors to overall systolic function of the ventricle, with the 100% thickening fraction of the posterior wall achieved by the timely shortening of the long axis that results in significant fattening of the segment during systole [9]. Our findings in the current study also remain consistent with the known time relations of shape change during isovolumic contraction (pre-ejection) in similar canine studies [10]. This coherent function has a significant implication on the energy transfer from the myocardium to the circulation. Our study elaborates on the pattern of the synchronous function of the two axes, by demonstrating a normal time delay between the shortening velocities of the two axes. This principle of asynchrony has been recently used in assessing patient suitability for cardiac resynchronization therapy [11]. However the main difference is the number of segments used (up to 16 in some studies) [12] rather than our simple model of two coordinate axes. Our data suggest a very close relationship between velocities of the two axes and the timing of LV pressure and aortic flow events. These timings of normal asynchrony at rest between the minor and long axes and their relations to pressure and flow events demonstrate that global function of the ventricle is likely to determine the overall stroke volume.

The observations that minor axis shortening velocity coincided with peak aortic velocity while long axis shortening velocity coincided with peak LV pressure are equivalent to the known complex phase relations of flow leading pressure drop in a fluidic system dominated by capacitance, i.e. vessel elasticity. Based on such system equivalence, further studies may demonstrate a coordinated reversal of these phase relationships during exercise states that would be characteristic of an inertance-dominated fluidic system. Furthermore, our analysis provides information on the third hemodynamic component: the aortic waves. Minor and long axis velocities each correlate closely with the arrival of the reflection waves and the onset of the expansion wave, respectively. As the arrival of reflected wave is associated with the onset of speed decline of LV minor axis in our data, we postulate that the reflected wave may have an effect on LV wall speed itself, however this is a question for a separate study. Reflected waves have been previously shown to have a significantly negative effect on subendocardial function in patients with peripheral arteriopathy during arterial clamping [13] and the close relationship between the extent of abbreviated ejection and filling time and clinical response to cardiac resynchronization therapy we have recently reported supports our current findings [14].

4.4. Clinical implications

With LV disease, prolonged early systolic shortening results in delayed onset of tension development and hence onset of ejection [14] Despite the impaired rate of pressure rise, the resulting transvalvular gradient opens the aortic valve and hence ejection follows. However, the end result is

abbreviated aortic ejection time despite a prolonged isovolumic contraction period (since timing of aortic closure remains unchanged), impingement of early diastolic filling due to post-systolic tension, and ultimately compromised stroke volume. This study highlights the fundamental basis of LV asynchrony and its effect on ejection time and systolic events in a 3-component manner; flow velocity, pressure, and wave intensity. Finally, our results are supported by recently published data in dogs which showed optimised global LV systolic function over broad regions of the lateral wall irrespective of the pacing lead position,[15] and hence independent of the regional function of the 16 segment model.

4.5. Limitation and future work

By evaluating only two dimensions this experiment investigates LV global movement, not segmental. There is known significant intersegmental heterogeneity to myocardial contraction. This experiment is also on normal LV. Applying the same techniques in asynchronous model of cardiomyopathy should provide more insight into the concept of LV asynchrony.

4.6. Conclusions

Normal long and minor axis asynchrony is implicit in supporting aortic pressure timing and hence stroke volume. Reproduction of this data in patients using available echocardiographic techniques should assist in identifying the most accurate measurements required for optimising ventricular synchronous function, as means of obtaining optimum stroke volume.

Acknowledgements

The authors of this manuscript have certified that they comply with the Principles of Ethical Publishing in the International Journal of Cardiology [16].

References

- [1] Henein MY, Gibson DG. Normal long axis function. *Heart* 1999;81: 111–3.
- [2] Jones CJH, Raposo L, Gibson DG. Functional importance of the long axis dynamics of the human left ventricle. *Br Heart J* 1990;63:215–20.
- [3] Parker KH, Jones CJH. Forwards and backwards running waves in the arteries: analysis using the method of characteristics. *J Biomech Eng* 1990;112:322–6.
- [4] Khir AW, O'Brien A, Gibbs JSR, Parker KH. Determination of wave speed and wave separation in the arteries. *J Biomech* 2001;34:1145–55.
- [5] Lin LIK. A note on the concordance correlation coefficient. *Biometrics* 2000;56:324–5.
- [6] Melbin J, Detweiler DK, Riffle RA, Noordergraaf A. Coherence of cardiac output with rate changes. *Am J Physiol* 1982 Oct;243(4): H499–504.
- [7] Wiggers CJ. The interpretation of the intraventricular pressure curve on the basis of rapidly summated fractionate contractions. *Am J Physiol* 1927;80:1–11.
- [8] Henein MY, Gibson DG. Abnormal subendocardial function in restrictive left ventricular disease. *Br Heart J* 1994 Sep;72(3):237–42.
- [9] Greenbaum RA, Gibson DG. Regional non-uniformity of left ventricular wall movement in man. *Br Heart J* 1981 Jan;45(1):29–34.
- [10] Rankin JS, McHale PA, ArentzenLing D, et al. The three-dimensional dynamic geometry of the left ventricle in the conscious dog. *Circ Res* 1976 Sep;39(3):304–13.
- [11] Yu CM, Zhang Q, Fung JW, et al. A novel tool to assess systolic asynchrony and identify responders of cardiac resynchronization therapy by tissue synchronization imaging. *J Am Coll Cardiol* 2005 Mar 1;45(5):677–84.
- [12] Kapetanakis S, Kearney MT, Siva A, et al. Real-time three-dimensional echocardiography: a novel technique to quantify global left ventricular mechanical dyssynchrony. *Circulation* 2005 Aug 16;112(7):992–1000.
- [13] Henein MY, Das SK, O'Sullivan C, et al. Effect of acute alterations in afterload on left ventricular function in patients with combined coronary artery and peripheral vascular disease. *Heart* 1996 Feb;75 (2):151–8.
- [14] Duncan AM, Lim E, Clague J, et al. Comparison of segmental and global markers of dyssynchrony in predicting clinical response to cardiac resynchronization. *Eur Heart J* 2006 Oct;27(20):2426–32.
- [15] Helm RH, Byrne M, Helm PA, et al. Three-dimensional mapping of optimal left ventricular pacing site for cardiac resynchronization. *Circulation* 2007 Feb 27;115(8):953–61.
- [16] Coats AJ. Ethical authorship and publishing. *Int J Cardiol* 2009;131: 149–50.